Journal of Power Sources 195 (2010) 6062–6068

Contents lists available at ScienceDirect

Journal of Power Sources

journal homepage: www.elsevier.com/locate/jpowsour

Oligo(ethylene glycol)-functionalized disiloxanes as electrolytes for lithium-ion batteries☆

Zhengcheng Zhang[a,*], Jian Dong[a], Robert West[b], Khalil Amine[a,**]

[a] Chemical Sciences and Engineering Division, Argonne National Laboratory, 9700 South Cass Avenue, Argonne, IL 60439, USA
[b] Organosilicon Research Center, Department of Chemistry, University of Wisconsin-Madison, 1101 University Avenue, Madison, WI 53706, USA

ARTICLE INFO

Article history:
Received 22 October 2009
Received in revised form
15 December 2009
Accepted 16 December 2009
Available online 23 December 2009

Keywords:
Lithium-ion batteries
Electrolytes
Functionalized disiloxanes
Thermal stability
Cycling performance

ABSTRACT

Functionalized disiloxane compounds were synthesized by attaching oligo(ethylene glycol) chains, $-(CH_2CH_2O)-_n$, $n = 2–7$, via hydrosilation, dehydrocoupling, and nucleophilic substitution reactions and were examined as non-aqueous electrolyte solvents in lithium-ion cells. The compounds were fully characterized by ^1H, ^{13}C, and ^{29}Si nuclear magnetic resonance (NMR) spectroscopy. Upon doping with lithium bis(oxalato)borate (LiBOB) or $LiPF_6$, the disiloxane electrolytes showed conductivities up to 6.2×10^{-4} S cm^{-1} at room temperature. The thermal behavior of the electrolytes was studied by differential scanning calorimetry, which revealed very low glass transition temperatures before and after LiBOB doping and much higher thermal stability compared to organic carbonate electrolytes. Cyclic voltammetry measurements showed that disiloxane-based electrolytes with 0.8 M LiBOB salt concentration are stable to 4.7 V. The LiBOB/disiloxane combinations were found to be good electrolytes for lithium-ion cells; unlike $LiPF_6$, LiBOB can provide a good passivation film on the graphite anode. The $LiPF_6$/disiloxane electrolyte was enabled in lithium-ion cells by adding 1 wt% vinyl ethylene carbonate (VEC). Full cell performance tests with $LiNi_{0.80}Co_{0.15}Al_{0.05}O_2$ as the cathode and mesocarbon microbead (MCMB) graphite as the anode show stable cyclability. The results demonstrate that disiloxane-based electrolytes have considerable potential as electrolytes for use in lithium-ion batteries.

1. Introduction

Designing new ion-conducting polymer materials has been at the heart of research in the field of lithium batteries over past years [1–5].

Recently, our research has focused on the development of a polysiloxane polymer electrolyte, including cyclic, linear, branched, and cross-linked siloxanes [6–22]. Polysiloxanes have relatively low glass transition temperatures due to the low bond rotation energies associated with the Si–O–Si units. The concept of combining stable, flexible siloxane chains with poly(ethylene oxide) (PEO) has led to the development of a variety of polymeric structures with the expressed aim of increasing conductivity. Over the last few years, polysiloxanes with comb [5], double-comb [6–8], cyclic [19], and cross-linked structures [11,13] have been synthesized and investigated as possible candidates for both liquid and solid polymer electrolytes. Recently, our investigations into liquid polymer electrolytes have been influenced by the concept that conductivity will generally increase as the glass transition temperature and viscosity of the electrolyte decrease [23]. We have found that when shorter ethylene glycol and shorter polysiloxane segments are employed, the conductivity increases. In this paper, we summarize the synthesis of a class of low viscosity compounds from disiloxane starting materials, with each compound containing only one or two oligo(ethylene glycol) chains. The conductivity, thermal properties, and the performance of lithium cells using these compounds as electrolyte solvents are presented.

2. Experimental

2.1. Materials

1,1,3,3-Tetramethyldisiloxane, 1,1,1,3,3-pentamethyldisiloxane, 1,1,1,3,3-pentamethylchlorodisiloxane, and 1,3-dichloro-1,1,3,3-tetramethyldisiloxane were purchased from Gelest. Tri(pentafluorophenyl)borane [$B(C_6F_5)_3$], Karstedt's catalyst solution [divinyltetramethyl-disiloxane Pt(0) complex, 3 wt% in

☆ The submitted manuscript has been created by UChicago Argonne, LLC, Operator of Argonne National Laboratory ("Argonne"). Argonne, a U.S. Department of Energy Office of Science laboratory, is operated under Contract No. DE-AC02-06CH11357. The U.S. Government retains for itself, and others acting on its behalf, a paid-up nonexclusive, irrevocable worldwide license in said article to reproduce, prepare derivative works, distribute copies to the public, and perform publicly and display publicly, by or on behalf of the Government.

* Corresponding author. Tel.: +1 630 252 7868; fax: +1 630 972 4440.
** Corresponding author. Tel.: +1 630 252 3838; fax: +1 630 972 4451.
E-mail addresses: zzhang@anl.gov (Z. Zhang), amine@anl.gov (K. Amine).

0378-7753/$ – see front matter © 2009 Elsevier B.V. All rights reserved.
doi:10.1016/j.jpowsour.2009.12.067

xylene], allyl bromide, vinyl ethylene carbonate (VEC), di(ethylene glycol) methyl ether, and tri(ethylene glycol) methyl ether were purchased from Aldrich. NaH (60% dispersion in mineral oil) was purchased from Acros Organics. Lithium bis(oxalato)borate (LiBOB) was supplied by Chemetall and was purified by recrystallization in dried, distilled acetonitrile (refluxed over CaH_2 for 24 h and distilled before use, Aldrich). Triethylamine and pyridine were purchased from Aldrich and distilled over CaH_2 prior to use. Toluene and tetrahydrofuran (THF) was dried over sodium and benzophenone.

2.2. Apparatus

^1H and ^{13}C NMR analyses of the samples were carried out on a Bruker AC300 spectrometer; ^{29}Si NMR analysis was performed on a Varian Unity 500 spectrometer using deuterated chloroform ($CDCl_3$, 99.8%, Aldrich) as the solvent. Viscosity measurements were performed on a Brookfield LVDV–I+ viscometer.

Conductivity experiments were conducted by pouring a disiloxane electrolyte inside a Teflon *O*-ring sandwiched between two stainless steel discs in a 2032 coin cell. Ionic conductivity was determined by the AC impedance method on a BAS-ZAHNER IM6 electrochemical analyzer (Gamry Instruments). Using a frequency range from 0.01 Hz to 1 MHz, the impedance was recorded over a temperature range from room temperature to 70 °C.

Differential scanning calorimetry (DSC) was employed for thermal data using a Perkin–Elmer Pyris Diamond instrument. The instrument was calibrated with heptane, mercury, and poly(dimethylsiloxane). All samples were loaded under dry argon. Because little difference was seen between samples that were cooled quickly from room temperature and those cooled slowly, undoped samples were simply cooled very quickly to −160 °C and heated from −160 °C to 200 °C at 10 °C min^{-1}. In all samples there were no transitions above 0 °C, so doped samples were heated to only 0 °C, all using a rate of 10 °C min^{-1}. The Pyris DSC software allowed mathematical computation of the onset of glass transition. Each sample was duplicated at least once.

The charge–discharge cycling performance was tested on a Maccor Electrochemical Analyzer using 2032 coin cells with $LiNi_{0.80}Co_{0.15}Al_{0.05}O_2$ as the cathode, MCMB graphite as the anode, and a Celgard trilayer (polypropylene/polyethylene/polypropylene) separator soaked with disiloxane electrolytes. A two-cycle formation step was applied prior to the cycling testing at the C/5 rate. Performance data were acquired and analyzed by the software associated with the instrument.

2.3. Synthesis

Synthesis of ***1a*** (*n* = 3): To a flame-dried, three-necked 50 mL flask was added 1,1,1,2,2-pentamethyldisiloxane (10.00 g, 0.067 mol) and tri(ethylene glycol) allyl methyl ether (16.50 g, 0.081 mol) by a syringe under argon. 50 μL Karstedt's catalyst solution was then injected into the solution under vigorous stirring. The reaction solution was then heated to and kept at 75 °C until no –Si–H peak was observed at 4.6 ppm in the ^1H NMR spectrum. The excess of tri(ethylene glycol) allyl methyl ether and its isomeric byproducts were removed by Kugelrohr distillation. The pure **1a** (*n* = 3) compound was obtained by fractional distillation under a vacuum of 0.1 torr with a yield of 92%. ^1H NMR ($CDCl_3$), δ (ppm) 3.45–3.63 (OCH_2CH_2O), 3.25–3.35 (OCH_3, CCH_2O), 1.53 (CCH_2C), 0.46 ($SiCH_2C$), −0.05 to 0.05 ($SiCH_3$). ^{13}C NMR ($CDCl_3$), δ (ppm) 73.9 (CCH_2O), 69.7–71.8 (OCH_2CH_2O), 58.7 (OCH_3), 23.0 (CCH_2C), 13.9 ($SiCH_2$), –0.5 to 1.0 ($SiCH_3$). ^{29}Si NMR ($CDCl_3$), δ (ppm) 6.1 ($(CH_3)_3SiO$), 6.4 ($(CH_3)_2CH_2SiO$)).

Synthesis of ***2a*** (*n* = 3): Similar reactions were carried out to synthesize **2a** (*n* = 3) by employing 1,1,3,3-tetramethyldisiloxane as starting material, and the stoichiometric ratio of disiloxane to oligoether was 1:2.4. ^1H NMR ($CDCl_3$), δ (ppm) 3.45–3.63 (OCH_2CH_2O), 3.25–3.35 (OCH_3, CCH_2O), 1.53 (CCH_2C), 0.46 ($SiCH_2C$), −0.05 to 0.05 ($SiCH_3$). ^{13}C NMR ($CDCl_3$), δ (ppm) 73.9 (CCH_2O), 69.7–71.8 (OCH_2CH_2O), 58.7 (OCH_3), 23.0 (CCH_2C), 13.9 ($SiCH_2$), −0.5 to 1.0 ($SiCH_3$). ^{29}Si NMR ($CDCl_3$), δ (ppm) 6.4 ($O(CH_3)_2SiCH_2-$)).

Synthesis of ***2b*** (*n* = 3): To a flame-dried 100 mL Schlenk flask were added 1,1,3,3-tetramethyldisiloxane (10.00 g, 0.074 mol), tri(ethylene glycol) methyl ether (26.86 g, 0.164 mol, vacuum distilled prior to use), and 40 mL dry toluene. To this clear solution was then added 0.038 g (0.05 mol% of Si–H) $B(C_6F_5)_3$. The reaction mixture was heated to and vigorously stirred at 80 °C, whereupon bubbling was observed. Aliquots were taken periodically for Fourier transform-infrared measurement until no peak was detected at 2170 cm^{-1}. When the reaction was complete, toluene and excess tri(ethylene glycol) methyl ether were removed by rotovap and Kugelrohr distillation to yield a colorless compound.

Synthesis of ***1b*** (*n* = 3): Similar reactions were carried out to synthesize **1b** (*n* = 3) by employing 1,1,13,3-pentamethyldisiloxane as starting material, and the stoichiometric ratio of disiloxane to oligoether was 1:1.1.

Synthesis of ***2b–2*** (*n* = 3): Tri(ethylene glycol) methyl ether (17.38 g, 0.106 mol), triethylamine (10.7 g, 0.106 mol), and anhydrous THF (40 mL) were syringed into a 100 mL flask placed in an ice water bath. 1,3-Dichloro-1,1,3,3-tetramethyldisiloxane (10.77 g, 0.053 mol, distilled prior to use) was then added dropwise to the solution while stirring. Upon complete addition, the solution was stirred at room temperature for 2 h, after which the reaction mixture was heated to 50 °C and kept at this temperature for 5 h. A white precipitate was filtered, and THF was removed by rotary evaporation. The crude product was then dissolved in toluene, and the excess of tri(ethylene glycol) methyl ether was extracted with small portions of water (five times) until no –OH signal at 3400 cm^{-1} was present in the infrared spectrum. Pure **2b–2** (*n* = 3) was obtained by fractional distillation, and its structure was confirmed by ^1H, ^{13}C, and ^{29}Si NMR.

Synthesis of ***1b–2*** (*n* = 3): Similar reactions were carried out to synthesize **1b–2** (*n* = 3) by employing 1,1,1,3,3-pentamethylchlorodisiloxane as starting material, and the stoichiometric ratio of disiloxane to oligoether was 1:1.1.

2.4. Preparation of disiloxane/LiBOB complexes

A stoichiometric amount of disiloxane was added to a LiBOB/THF solution in an argon-filled glove box. After magnetically stirring, the resulting solution was evacuated for 12 h and then further evacuated on a high-vacuum line (~10^{-7} torr) for 24 h to completely remove the THF. The complexes were then loaded into a button cell for conductivity measurement.

2.5. Conductivity measurements

Procedures involving the building of cells were carried out in an argon-filled dry box. The disiloxane electrolytes were prepared by doping the polymers with LiBOB in a THF solution under dry, inert conditions. The solvent was removed under vacuum on a Schlenk line once a homogeneous mixture was achieved. The sample was then placed under high vacuum (<10^{-7} torr) for 24 h. Doping levels are reported as the ratio of ethyl oxide groups (EO) per lithium cation (Li^+). The oxygens associated with the disiloxane "backbone" are not included in this ratio.

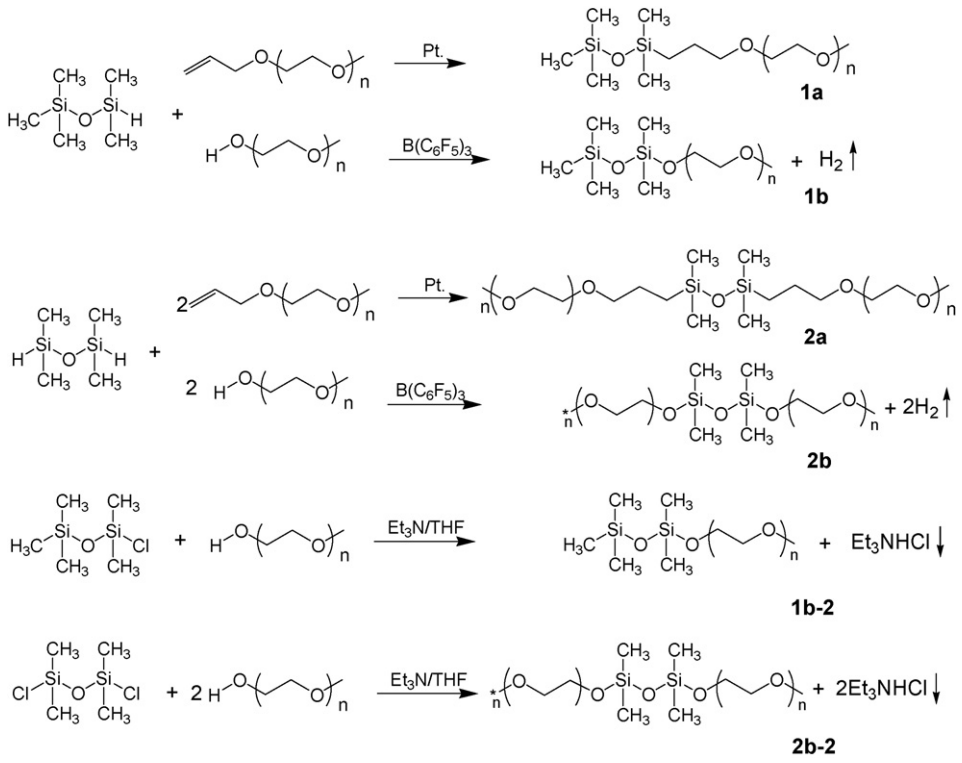

Scheme 1. Synthesis of oligo(ethylene glycol)-functionalized disiloxanes.

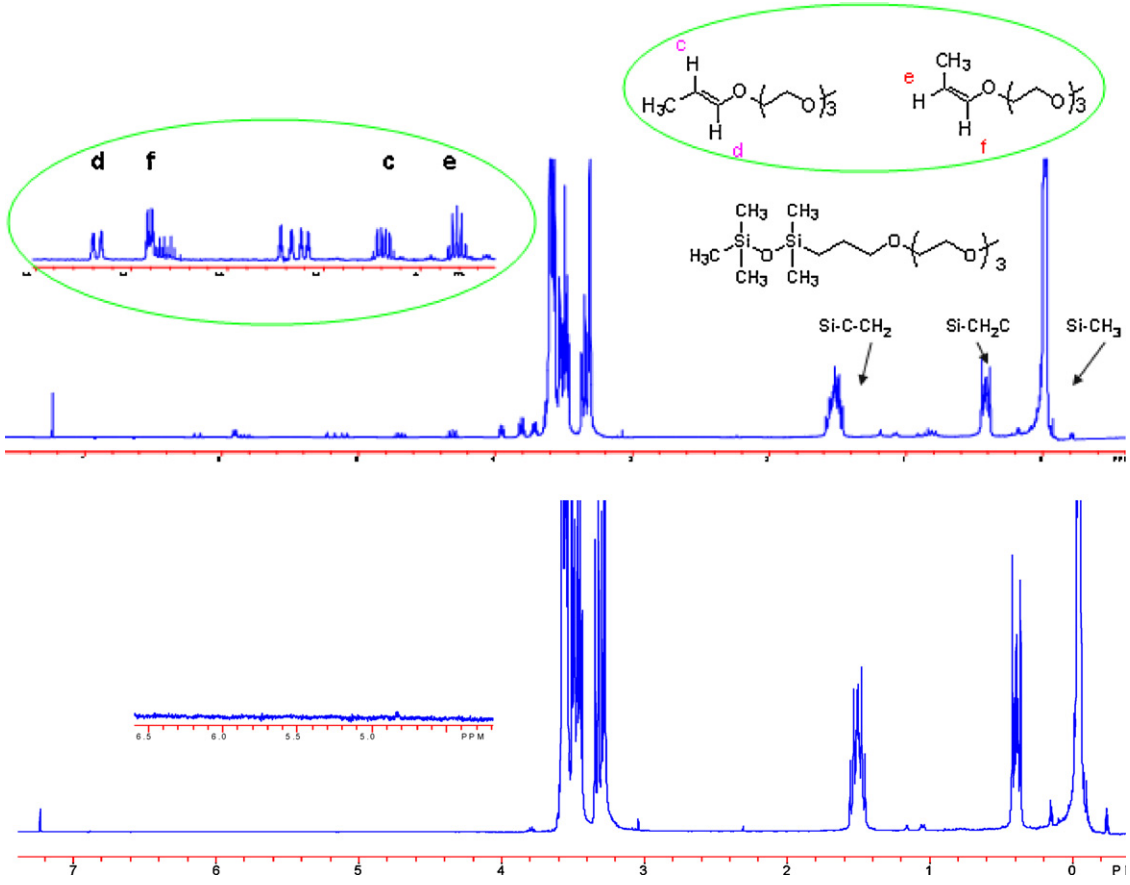

Fig. 1. ^{1}H NMR of the **1a** (n = 3) before and after purification.

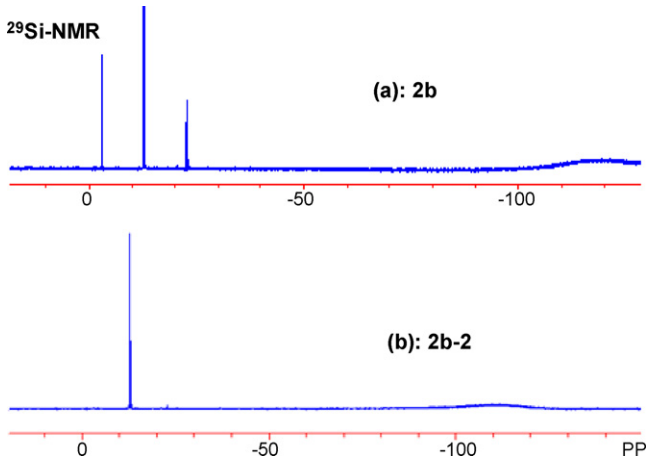

Fig. 2. ^{29}Si NMR of **2b** (n = 3) (a, top) and **2b–2** (b, bottom).

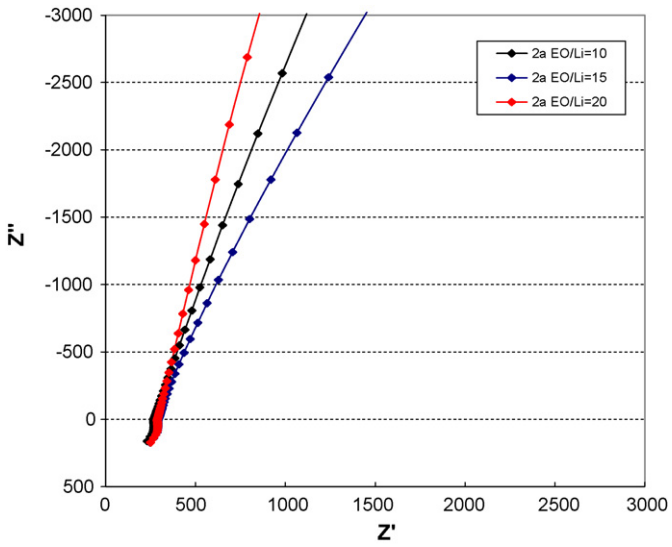

Fig. 3. Nyquist plots of disiloxane 2a/LiBOB complexes with [Ethylene oxide]/[Li$^+$] = 10, 15 and 20.

3. Results and discussion

3.1. Disiloxane synthesis and purification

The synthesis of a series of oligo(ethylene glycol) functionalized disiloxanes is summarized in Scheme 1. These disiloxane compounds contain the smallest Si–O–Si "backbone" for the purpose of molecular flexibility. In compounds **1a** and **2a**, the disiloxanes were bonded to oligoether chain(s) through a (–$CH_2CH_2CH_2$–) using a platinum-catalyzed hydrosilylation reaction. Similar to the synthesis of their polymeric analogs, isomers (*cis*- and *trans*-) of tri(ethylene glycol) allyl methyl ether generated as byproducts in the catalytic cycle were detected by ^{1}H NMR spectra, as shown in Fig. 1. The formation of olefin isomers can be attributed to the dissociation of the labile divinyltetramethyl-disiloxane ligand and the subsequent generation of colloidal Pt species [24–26], leading to undesired side products and coloration of the product. It is estimated that up to 20% isomers exist in the reaction mixture; therefore, a 20% excess of tri(ethylene glycol) allyl methyl ether was employed in the synthesis of **1a** and **2a** series to ensure the complete conversion of Si–H.

For synthesis of products of disiloxanes directly bonded to oligoether chain(s), two synthetic routes were employed. In the first synthesis trial, a $B(C_6F_5)_3$-catalyzed dehydrocoupling reaction was used to make **1b** and **2b**. However, it was noted that side reactions occurred, as evidenced by the ^{29}Si NMR spectrum. For example, in addition to the desired peak at −30 ppm for **2b**, two extra peaks were detected at −51 ppm and −68 ppm (Fig. 2a), which are characteristic of the M unit and T unit, respectively. To avoid the redistribution of the disiloxane backbone, an alternative synthetic route was employed in which 1-chloro-1,1,3,3,3,-pentamethyldisiloxane and 1,2-dichloro-1,1,3,3-tetramethyldisiloxane were used as the starting disiloxane materials for synthesis of **1b–2** and **2b–2** (Scheme 1). ^{29}Si NMR spectra of the disiloxanes **2b–2** prepared by the new method (Fig. 2b) showed a single peak, indicating that Si–O–Si rearrangement does not occur via this reaction pathway.

A high level of purity was achieved since these compounds have relatively low boiling points. Under reduced pressure, disiloxanes of **1a**, **2a**, **1b–2**, and **2b–2** are distillable and, therefore, can be efficiently separated from impurities (e.g., byproducts and starting material as shown in Fig. 1). Distillation of the compounds yielded clear, colorless liquids, which were analyzed by ^{1}H, ^{13}C, and ^{29}Si NMR. In the cases where the final product had a relatively high boiling point and could not be distilled (such as the di-substituted disiloxane compounds containing oligoether chains with 5–7 repeat units), refluxing over activated charcoal was carried out to decolorize the product **2a** (n = 5, 6, or 7) and remove the remaining residual catalyst. Compounds **2b–2** (n = 5, 6, or 7) were also purified by removing unreacted starting material by solvent extraction.

3.2. Disiloxane conductivity

The ionic conductivity of the synthesized disiloxanes was studied employing LiBOB as a lithium salt. LiBOB fulfills the complete set of stringent requirements essential for lithium-ion cell applications and is being widely investigated as a lithium salt and electrolyte additive [27–29]. LiBOB is soluble in all synthesized disiloxanes, and the resulting complexes are completely amorphous. The doped samples became viscous but remain liquids due to the low molecular weight of the disiloxanes. The Nyquist plots, measured by AC impedance method over the frequency range of 1 Hz to 1 M Hz, were described in an equivalent circuit of a parallel capacitance and resistance (see Fig. 3). Ionic conductivities for disiloxane/LiBOB complexes are summarized in Table 1.

Table 1
Conductivity (σ), glass transition temperature (T_g), activation energy (E_a), and viscosity (μ) of disiloxane/LiBOB electrolytes.

Sample	**2b–2** (n = 3)	**2b–2** (n = 3)	**2a** (n = 3)	**2a** (n = 3)	**1a** (n = 3)	**1b–2** (n = 3)
EO/Li	10:1	20:1	10:1	10:1	10:1	10:1
σ (S cm^{-1}, 25 °C)	5.2×10^{-4}	5.5×10^{-4}	2.5×10^{-4}	3.4×10^{-4}	4.67×10^{-4}	6.2×10^{-4}
T_g (°C)	−93.0	−98.8	−74.7	−88.6	−82.7	−103.0
T_0 (°C)	−103	−86.0	−60.6	−96.2	−75.6	−90.2
E_a (kJ mol^{-1})	6.39	3.55	5.02	3.52	4.25	5.40
μ (cP, 25 °C)[a]	4.10	–	6.00	–	3.80	1.20

[a] Solvent only.

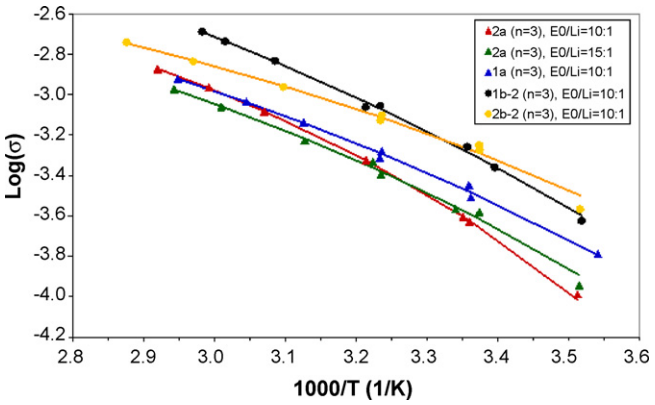

Fig. 4. Conductivity vs temperature of **1a**, **2a**, **1b–2**, and **2b–2** at LiBOB doping level of [ethylene oxide]/[Li^+] = 10:1 and 15:1.

As predicted from its relatively low molecular weight, low glass transition temperature, low viscosity, and lack of crystalline transitions, the disiloxane compounds show much higher conductivities than their polymeric analogs reported previously, although less conductive than the oligoether-substituted silanes reported elsewhere [30]. The most conductive disiloxane/LiBOB complex, and also one of the least viscous, was **1b–2**. It contains one tri(ethylene glycol) chain directly coupled with a Si atom and has a conductivity of 6.2×10^{-4} S cm^{-1} at room temperature. The relatively low viscosity of this electrolyte could account for its high conductivity. The disiloxane compounds with a $(CH_2)_3$ spacer mounted between the oligoether chain and the siloxane exhibited lower conductivity at all measured temperatures, as illustrated in Fig. 4. Among all the synthesized disiloxanes, 1a shows the highest conductivity for a spacer-type disiloxane-based electrolyte: 4.67×10^{-4} S cm^{-1} at 25 °C and 6.45×10^{-4} S cm^{-1} at 37 °C. Interestingly, disiloxane **2b** synthesized by the dehydrocoupling reaction exhibited a twofold increase in conductivity compared with its pure version **2b–2**. This result agrees with the analysis of the ^{29}Si NMR spectrum showing that fragmentation occurs during the synthesis of **2b** forming the monosilicon species (as evidenced by NMR data) as a side product. The low viscosity (Table 1), caused by the presence of such a compound, accounts for the increase of its conductivity.

Arrhenius plots of disiloxane/LiBOB complexes as shown in Fig. 4 are all curved, suggesting that oligomeric chains contribute to ion transport as a polymer would, rather than as has been previously shown for Li-ion conducting liquid electrolytes [23]. Note that the optimal conductivity of disiloxanes varies with temperature and doping level. As an example, compound **2b–2** has optimum conductivity for 25 °C at the 20:1 doping level and for 37 °C at the 10:1 doping level (Table 1). The conductivities of 5.5×10^{-4} S cm^{-1} for 20:1 at 25 °C and 8.9×10^{-4} S cm^{-1} for 10:1 at 37 °C are the highest reported for mono-comb polysiloxane electrolytes.

The Vogel–Tamman–Fulcher (VTF) equation: $\sigma = AT^{-1/2} \exp(-B/(T - T_0))$ has been used to fit the behavior of the temperature-dependant conductivities of these oligomeric electrolytes. Table 1 lists the values of E_a, the apparent activation energy, and T_0, the ideal glass transition temperature. The T_0 values are all closer to the experimental T_g than the typical 50 K below T_g. Unlike Hooper et al. [7,8], who found that conductivity increased with higher activation energy, or Lyons et al. [18], who found that conductivity decreased with higher activation energy, we saw no apparent trend. The activation energy may be so small that bond rotation at the investigated temperatures readily occurs; thus, this parameter is no longer an obstacle to conductivity.

The trend that conductivity increased with decreasing glass transition temperature was observed for disiloxane compounds, as shown in Fig. 5. Di-substituted spacer type disiloxane **2a** has the highest T_g of −97.6 °C, and **1b–2**, with a T_g of −114.0 °C, was our most conductive disiloxane.

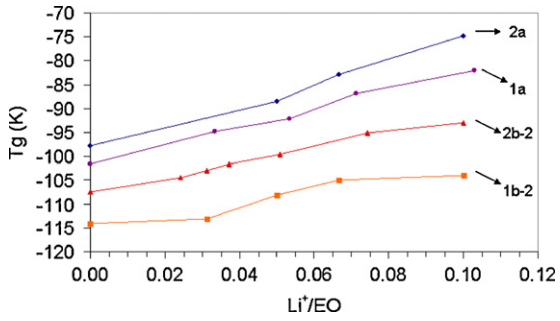

Fig. 5. Onset glass transition temperatures of disiloxanes at various doping levels.

3.3. Disiloxane thermal stability

Fig. 6 compares DSC data of 0.8 M LiBOB in **1a**, **2a**, and **2b–2** electrolyte with data for a conventional 1.0 M $LiPF_6$ in ethylene carbonate (EC):dimethyl carbonate (DMC) (1:1 weight ratio) electrolyte. While the conventional electrolyte shows decomposition reactions that generate a significant amount of heat around 260 °C, disiloxane/LiBOB electrolyte shows no decomposition or heat generation up to 350 °C. This result clearly demonstrates that these new disiloxane-based electrolytes have high thermal stability and may provide better safety characteristics than conventional organic carbonate-based electrolytes.

Flammability tests were also carried out on the disiloxane/LiBOB electrolyte. In these tests, a glass wick was initially soaked with disiloxane electrolyte; thereafter, one tip of the wick was ignited, and the flame propagation rate along the wick was monitored. The results indicated that the new electrolytes produced a flame propagation rate of less than 35 mm min^{-1} and had self-extinguishing characteristics, whereas the conventional $LiPF_6$/EC:DEC (1:1) electrolyte produced a violent flame with a significantly higher propagation rate (>1000 mm min^{-1}).

3.4. Disiloxane electrochemical stability

Electrochemical cells were assembled with Pt/Li/Li electrodes and the disiloxane/LiBOB electrolyte and were subjected to cyclic

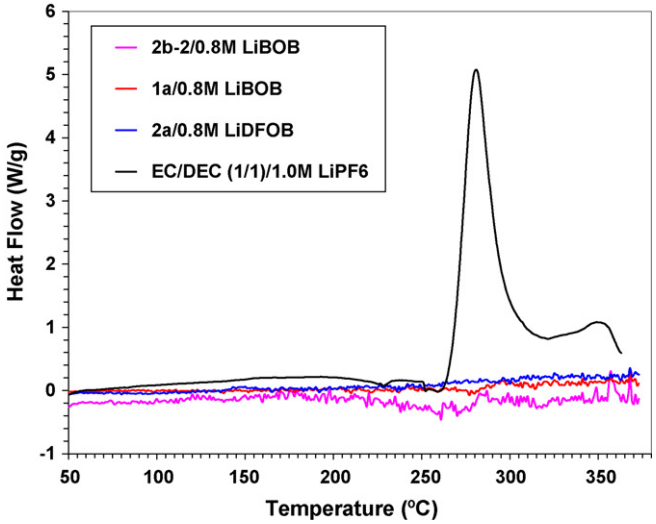

Fig. 6. Differential scanning calorimetry curves for electrolytes of 0.8 M LiBOB/disiloxanes and 1.0 M $LiPF_6$/EC:DEC (1:1).

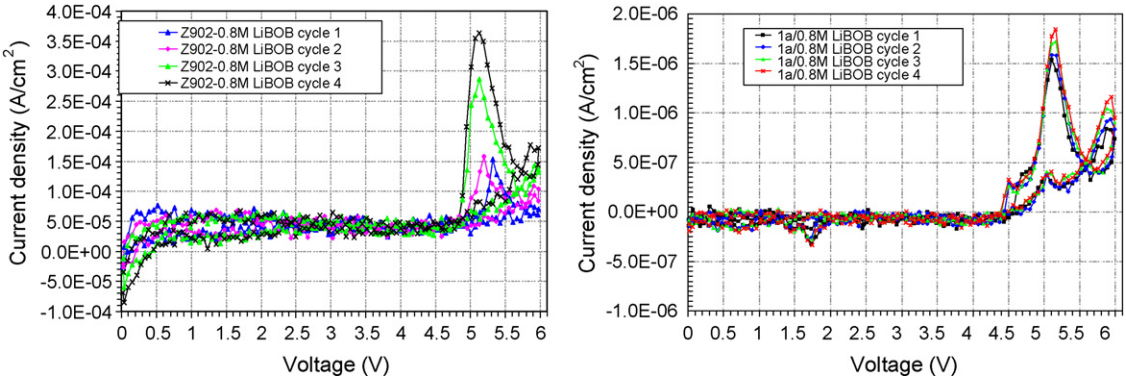

Fig. 7. Cyclic voltammetry curves for disiloxane/LiBOB electrolytes: 0.8 M LiBOB–**2b**–**2** (left) and 0.8 M LiBOB–**2a** (right).

voltammetry at 50 mV/s. The resultant voltammograms over four cycles are shown in Fig. 7. The non-spacer disiloxane **2b**–**2** has a high electrochemical window up to 4.7 V, while the spacer-type disiloxane **2a** is slightly lower (4.5 V). These results show that disiloxane electrolytes exhibit good electrochemical stability, comparable to conventional electrolytes.

3.5. Disiloxane rate capability

The rate capabilities of disiloxane electrolytes were evaluated by charging lithium-ion cells (3.0 mAh capacity) with a constant current equivalent to C/20 rate to 4.0 V, followed by a constant voltage charge with a cutoff current equivalent to C/100. The cells were then discharged to 2.7 V at constant currents of C/10, C/5, C/1, 1C, and 2C. As shown in Fig. 8, the disiloxane **1a**/0.8 M LiBOB cells demonstrated high capacity retention at the C/2, C/5, and C/10 rates. Although only 20% capacity was retained at the 2C rate, the cell still retained greater than 50% capacity when discharged at 1C.

3.6. Disiloxane cycling performance

Fig. 9 shows the positive electrode specific charge/discharge capacities vs cycle number for a lithium-ion cell with a 0.8 M LiBOB/**2b**–**2** electrolyte, a $LiNi_{0.8}Co_{0.15}Al_{0.05}O_2$ cathode, and a MCMB graphite anode. The cell was charged and discharged at the C/5 rate. When discharged over 3.0–4.0 V and 3.2–3.9 V, the cell performed extremely well with 100% efficiency and showed no capacity fade after 100 cycles. The capacity fading when cycled over 3.0–4.1 V is attributed to the growing SEI formed by the continuous decomposition of LiBOB on the surface of the graphite at higher voltage.

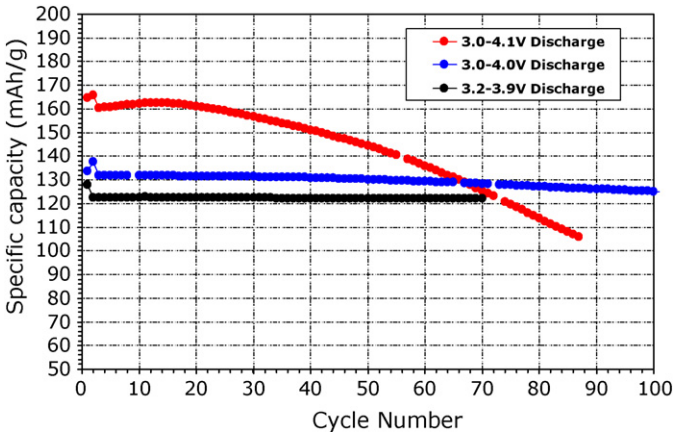

Fig. 9. Positive electrode specific discharge capacities vs cycle number for coin cells $LiNi_{0.80}Co_{0.15}Al_{0.05}O_2$/0.8 M LiBOB–**2b**–**2**/MCMB cycled between 3.0–4.1 V, 3.0–4.0 V and 3.2–3.9 V.

We chose LiBOB as the lithium salt because it provides an effective passivation film on the carbon anode, as supported by the data in Fig. 8. To explore the compatibility of disiloxanes with

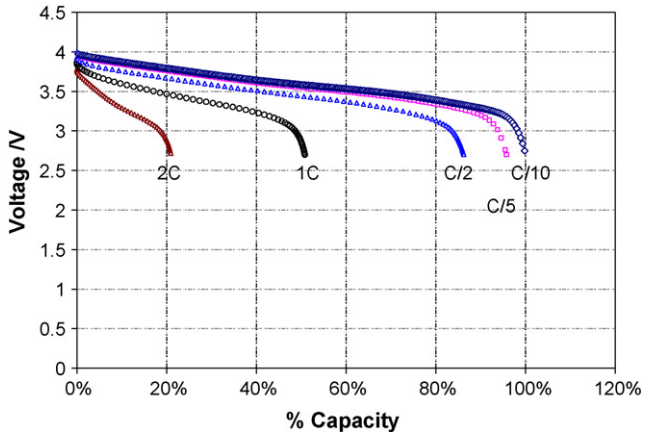

Fig. 8. Discharge profiles of coin cells $LiNi_{0.80}Co_{0.15}Al_{0.05}O_2$/**1a**–0.8 M LiBOB/MCMB (the cell capacity is 2.2 mAh; charge the cells with a current of C/20 to 4.0 V with cutoff current of C/100, then discharge the cells with a current of C/10, C/5, C/2, 1C, 2C to 2.7 V).

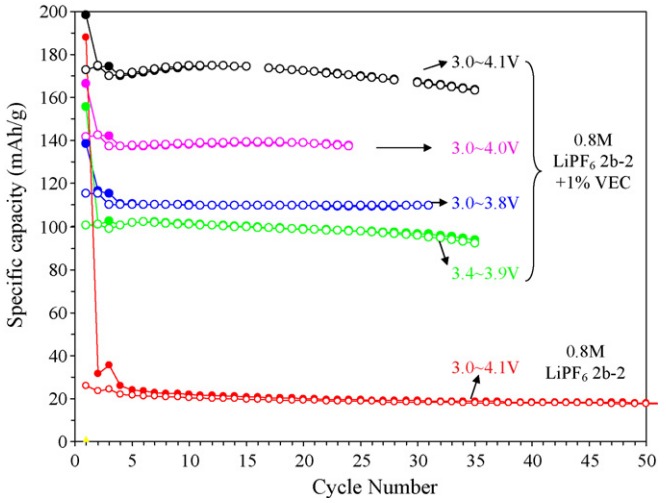

Fig. 10. Positive electrode specific charge/discharge capacities vs cycle number for coin cells $LiNi_{0.80}Co_{0.15}Al_{0.05}O_2$/0.8 M $LiPF_6$–**2b**–**2** + 1 wt% VEC/MCMB at different charging voltage ranges.

$LiPF_6$, the conventional lithium salt, 0.8 M electrolyte was prepared by dissolving $LiPF_6$ in disiloxane **2b–2** and was used as electrolyte for lithium-ion cells with MCMB graphite as the anode and $LiNi_{0.8}Co_{0.15}Al_{0.05}O_2$ as the cathode. As shown in Fig. 10, the specific capacities surprisingly suffered from a dramatic fade from the very first charge and discharge, indicating the lack of an integrated SEI film on the anode surface. However, when 1 wt% VEC was added, the **2b–2**/0.8 M $LiPF_6$ electrolyte could be cycled without significant capacity fade, even between 3.0 V and 4.1 V. This improvement occurred through the formation of a favorable SEI film on the anode surface. Note that the cells with 0.8 M $LiPF_6$–**2b–2** + 1 wt% VEC exhibited higher specific capacities than those with 0.8 M LiBOB–**2b–2** electrolyte cycled in the same voltage range. For example, when cycled over 3.0–4.0 V, the achieved specific capacity for the 0.8 M $LiPF_6$–**2b–2** + 1 wt% VEC was 140 mAh/g, compared with 130 mAh for 0.8 M LiBOB–**2b–2**. This result indicates that the disiloxane electrolytes, even when combined with a reactive, highly oxidizing cathode, such as $LiNi_{0.80}Co_{0.15}Al_{0.05}O_2$, can provide good cycle and calendar life characteristics.

4. Conclusions

The oligo(ethylene glycol) functionalized disiloxanes **1a**, **2a**, **1b**, **1b–2**, **2b**, and **2b–2** with various chain lengths were synthesized, purified, and fully characterized by NMR spectroscopy as non-aqueous electrolyte for lithium-ion batteries. The disiloxane electrolyte studied in this work affords high purity with very low viscosity, less than 6 cP. The DSC results clearly indicate that these new electrolytes are extremely stable. Their complexes with LiBOB were investigated as the electrolyte for lithium-ion batteries. A stable SEI layer was formed on the MCMB graphite anode in the disiloxane/LiBOB electrolytes, but was not obtained in disiloxane/$LiPF_6$ electrolyte. The cell performance was significant improved by adding 1 wt% VEC to the disiloxane/$LiPF_6$ electrolyte. Further testing demonstrated that these functionalized disiloxanes can be used as thermally and electrochemically stable electrolyte solvents for lithium-ion batteries. These electrolytes, which are not as flammable as conventional organic carbonate-based solvents, show outstanding charge/discharge cycling behavior in lithium-ion cells with a MCMB graphite anode and a $LiNi_{0.80}Co_{0.15}Al_{0.05}O_2$ cathode.

Acknowledgments

This work was supported by the U.S. Department of Commerce, National Institute of Standards and Technology, and Advanced Technology Program. Argonne National Laboratory, a U.S. Department of Energy Office of Science laboratory, is operated under Contract No. DE-AC02-06CH11357.

References

[1] M.B. Armand, J.M. Chabagno, M. Duclot, Extended Abstracts, 2nd Int. Meeting on Solid Electrolytes, St. Andrews, Scotland, 1978.
[2] P.M. Blonsky, D.F. Shriver, H.R. Allcock, P. Austin, J. Am. Chem. Soc. 106 (1984) 6854.
[3] H.R. Allcock, R. Prange, T.J. Hartle, Macromolecules 34 (2001) 5463.
[4] R. Spindler, D.F. Shriver, J. Am. Chem. Soc. 110 (1988) 3036.
[5] E. Morales, J.L. Acosta, Electrochim. Acta 45 (1999) 1049.
[6] R. Hooper, L.J. Lyons, D.A. Moline, R. West, Silicon Chem. 1 (2002) 121.
[7] R. Hooper, L.J. Lyons, M.K. Mapes, D. Schumacher, D.A. Moline, R. West, Macromolecules 34 (2001) 931.
[8] R. Hooper, L.J. Lyons, D.A. Moline, R. West, Organometallics 18 (1999) 3249.
[9] Z.C. Zhang, A. Simon, J.J. Jin, L.J. Lyons, K. Amine, R. West, Polym. Mater.: Sci. Eng. 91 (2004) 587.
[10] Z.C. Zhang, L.J. Lyons, K. Amine, R. West, Polym. Prepr. 45 (2004) 583.
[11] Z.C. Zhang, D. Sherlock, R. West, L.J. Lyons, K. Amine, R. West, Macromolecules 36 (2003) 917.
[12] Z. Zhang, L.J. Lyons, K. Amine, R. West, Macromolecules 28 (2005) 5714.
[13] Z.C. Zhang, J.J. Jin, F. Bautista, L.J. Lyons, N. Shariatzadeh, D. Sherlock, K. Amine, R. West, Solid State Ionics 170 (2004) 233.
[14] Z.C. Zhang, N.A.A. Rossi, L.J. Lyons, K. Amine, R. West, Polym. Prepr. 45 (2004) 700.
[15] N.A.A. Rossi, Z. Zhang, Q. Wang, K. Amine, R. West, Polym. Prepr. 46 (2005) 723.
[16] Z. Zhang, N.A.A. Rossi, A. Simon, C. Olson, Q. Wang, K. Amine, R. West, Polym. Prepr. 46 (2005) 662.
[17] N.A.A. Rossi, Z. Zhang, Q. Wang, K. Amine, R. West, Polym. Mater.: Sci. Eng. 92 (2005) 426.
[18] L.J. Lyons, K. Morcom, Y. Schneider, Z. Zhang, N.A.A. Rossi, R. West, Polym. Mater.: Sci. Eng. 92 (2005) 443.
[19] Z. Zhang, L.J. Lyons, J.J. Jin, K. Amine, R. West, Chem. Mater. 17 (2005) 5646.
[20] N.A.A. Rossi, Z. Zhang, Y. Schneider, K. Morcom, L.J. Lyons, Q. Wang, K. Amine, R. West, Chem. Mater. 18 (2006) 1298.
[21] L. Zhang, Z. Zhang, S. Harring, M. Straughan, R. Butorac, L. Lyons, Z. Chen, K. Amine, R. West, J. Mater. Chem. 18 (2008) 3713.
[22] Z. Chen, H. Wang, D. Vissers, L. Zhang, R. West, L. Lyons, K. Amine, J. Phys. Chem. C 112 (2008) 2210.
[23] G.Y. Gu, R. Laura, K.M. Abraham, Electrochem. Solid-State Lett. 2 (10) (1999) 486.
[24] I.E. Marko, S. Sterin, O. Buisine, G. Mignani, P. Branlard, B. Tinant, J.-P. Declercq, Science 298 (2002) 204.
[25] A.J. Arduengo, S.F. Gamper, J.C. Calabrese, F. Davidson, J. Am. Chem. Soc. 116 (1994) 4391.
[26] P.L. Arnold, F.G.N. Cloke, T. Geldbach, P.B. Hitchcock, Organometallics 18 (1999) 3228.
[27] U. Lischka, U. Wietelmann, M. Wegner, DE 19829030 C1 (1999).
[28] K. Xu, S. Zhang, T.R. Jow, W. Xu, C.A. Angell, Electrochem. Solid-State Lett. 5 (2002) A26.
[29] K. Xu, S. Zhang, T.R. Jow, Electrochem. Solid-State Lett. 6 (2003) A117.
[30] K. Amine, Q. Wang, D.R. Vissers, Z. Zhang, N.A.A. Rossi, R. West, Electrochem. Commun. 8 (2006) 429.